DOI: 10.1002/chem.200600835

Synthesis, Structures, and Properties of *meso*-Phosphorylporphyrins: Self-Organization through P–Oxo–Zinc Coordination

Yoshihiro Matano,*[a] Kazuaki Matsumoto,[a] Yukiko Terasaka,[a] Hiroki Hotta,[b] Yasuyuki Araki,[c] Osamu Ito,[c] Motoo Shiro,[d] Takahiro Sasamori,[e] Norihiro Tokitoh,[e] and Hiroshi Imahori[a]

Abstract: The synthesis, structures, and optical and electrochemical properties of *meso*-phosphorylporphyrins are described. The copper-catalyzed carbon–phosphorus cross-coupling reaction of a *meso*-iodoporphyrin with di-*n*-butyl phosphite and diphenylphosphane oxide has proved to be an efficient and general method for the synthesis of *meso*-phosphorylporphyrins. Zinc phosphorylporphyrins thus obtained readily undergo self-organization through P–oxo–Zn coordination to form noncovalently linked, cofacial porphyrin dimers or linear oligomers, which have been characterized by spectroscopic methods and X-ray crystallographic analyses. In toluene, CH_2Cl_2, and $CHCl_3$, the zinc phosphorylporphyrins exist mostly as dimers or monomers, depending on their concentrations, the temperature, and the presence of additives. The self-association constants for dimerization in toluene have been determined by UV/Vis absorption titration measurements. The *meso*-diphenylphosphorylporphyrin dimer displays excitonic coupling of the Soret band with a splitting energy of 940 cm^{-1}. Fluorescence lifetimes of the zinc phosphorylporphyrins have been found to be affected only slightly by the concentration of the solution, and by the addition of triphenylphosphane oxide, suggesting that the effect of dimerization on their photodynamics in the S_1 state is negligible. On the other hand, the effect of dimerization is clearly reflected in their electrochemical oxidation processes, as the initially produced radical cations are efficiently delocalized over the two porphyrin rings. These findings demonstrate the potential utility of *meso*-phosphorylporphyrins as new models for the special pair in photosynthesis and as new building blocks for porphyrin-based supramolecular materials.

Keywords: cross-coupling · P–O compounds · porphyrinoids · self-assembly · X-ray diffraction

Introduction

Metal–ligand coordinative interactions play an important role in the construction of porphyrin assemblies, and have been the subject of numerous studies in supramolecular, biomimetic, and materials chemistry.[1] In order to control the optical and electrochemical properties of such porphyrin assemblies, it is necessary to organize the chromophores into well-defined supramolecular architectures. In this context, much effort has been devoted to the design of new classes of peripheral substituents as coordination sites for metalloporphyrins. Among them, nitrogen bases such as pyridyl,[2] imidazolyl,[3] aminopyrimidyl,[4] and amino[5] groups are the most frequently used ligands to construct cofacial, linear, branched, cyclic, dendritic, and polymeric metalloporphyrin assemblies, in which the directional angle and basicity of the lone pair as well as the steric factors of the substituents define the structures and stabilities of the assemblies. Hydroxyl and carbonyl functions have also been used for the

[a] Prof. Y. Matano, K. Matsumoto, Y. Terasaka, Prof. H. Imahori
Department of Molecular Engineering
Graduate School of Engineering, Kyoto University
Nishikyo-ku, Kyoto 615-8510 (Japan)
Fax: (+81) 75-383-2571
E-mail: matano@scl.kyoto-u.ac.jp

[b] Dr. H. Hotta
Department of Chemistry, Faculty of Engineering
Gunma University
Kiryu 376-8515 (Japan)

[c] Dr. Y. Araki, Prof. O. Ito
Institute of Multidisciplinary Research for Advanced Materials
Tohoku University, Aoba-ku, Sendai 980-8577 (Japan)

[d] Dr. M. Shiro
Rigaku Corporation
Akishima-shi, Tokyo 196-8666 (Japan)

[e] Dr. T. Sasamori, Prof. N. Tokitoh
Institute of Chemical Research, Kyoto University
Uji, Kyoto 611-0011 (Japan)

Supporting information for this article is available on the WWW under http://www.chemeurj.org/ or from the author.

self-assembly of metalloporphyrins[6] and chlorophylls[7] as models for chlorosomal antennae in green photosynthetic bacteria. However, the potential utilities of other classes of ligands have not been fully addressed.[8]

Phosphorus-based functional groups are attractive candidates as peripheral ligands, because they provide a variety of coordination modes depending on the oxidation state and geometry of the phosphorus center. For example, trivalent σ^3-phosphorus groups act as typical P ligands, while pentavalent σ^4-phosphorus groups bearing a P–oxo bond behave as O ligands. In each case, the coordinating ability of the phosphorus or the P-bound heteroatom center is easily controlled by appropriate choice of substituents. Recently, Sanders and co-workers reported several types of linear porphyrin arrays, in which trivalent *meso*-phosphinophenyl and phosphinoethynyl groups were coordinated to the metal centers through their phosphorus donors (P–M; M = Ru, Rh).[9] On the other hand, the literature contains no examples of metalloporphyrin assemblies utilizing pentavalent phosphorus functionalities, and their potential utilities still remain to be clarified.

For reciprocal communication between the phosphorus substituent and the porphyrin π system, it is desirable to attach the phosphorus functional groups directly to the peripheral positions of the porphyrin ring. To the best of our knowledge, however, there is only limited information on peripheral carbon–phosphorus bond-forming reactions. In 1977, Evans and Smith reported that electrolysis of a mixture of tetraphenylporphyrin and triphenylphosphane afforded a β-(triphenylphosphonio)porphyrin.[10] Although this method has been applied to the synthesis of some *meso*- and β-phosphonioporphyrins,[11] no attention has been paid to other C–P bond-forming reactions. In recent years, transition-metal-catalyzed cross-coupling reactions of halogenated porphyrins with carbon[12] and heteroatom[13] nucleophiles have proved to be reliable methods for introducing a wide range of substituents such as aryl, heteroaryl, alkenyl, alkynyl, alkoxy, amido, and sulfanyl groups on the porphyrin ring. With this in mind, we decided to 1) establish a general method for peripheral carbon–phosphorus bond formation based on cross-coupling methodology, 2) elucidate the structures and properties of the P-substituted porphyrins, and 3) utilize them as new building blocks for supramolecular porphyrin assemblies. As a first target, we chose phosphoryl ($R_2P(O)$-) groups, which are expected to behave as neutral O ligands derived from polarized P–oxo bonds.

Herein, we report the synthesis, structures, and properties of *meso*-phosphorylporphyrins, which have been prepared by copper-catalyzed carbon–phosphorus cross-coupling reactions.[14] The zinc phosphorylporphyrins thus obtained have been found to undergo self-organization through P–oxo–Zn coordination to form cofacial porphyrin dimers or oligomers. In both types of aggregates, the σ^4-phosphorus center with a polarized P–oxo bond defines the orientation and distances of the porphyrin chromophores. The crystal structures, photophysical properties, and electrochemical properties of the zinc phosphorylporphyrin aggregates have been elucidated by means of X-ray crystallography, absorption and fluorescence spectroscopies, and cyclic voltammetry. The results obtained demonstrate the potential utility of phosphoryl groups as new peripheral coordinating sites for the formation of porphyrin-based supramolecules.

Results and Discussion

Synthesis and characterization of phosphorylporphyrins: Cross-coupling methodology has been successfully applied to peripheral carbon–phosphorus bond formation. Scheme 1

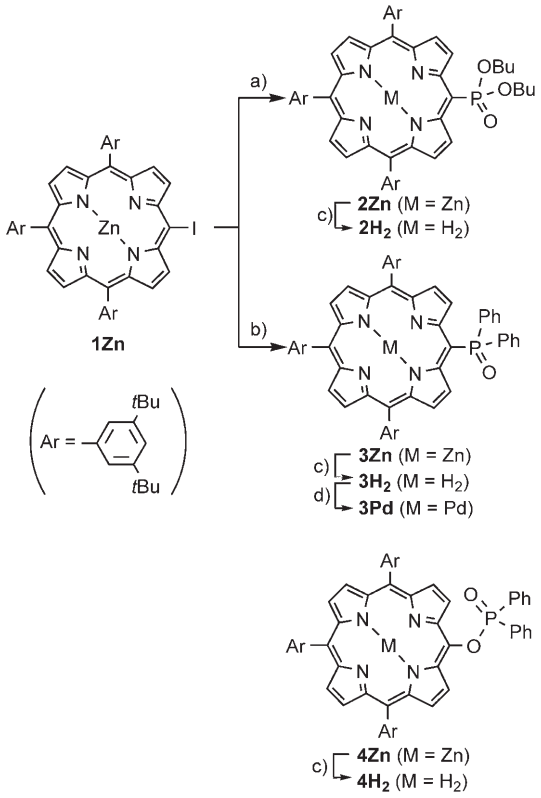

Scheme 1. Synthesis of *meso*-phosphorylporphyrins. Reagents and conditions: a) $HP(O)(OBu)_2$, CuI (20 mol%), Cs_2CO_3, $MeNH(CH_2)_2NHMe$, toluene, reflux; 81%. b) $Ph_2P(O)H$, CuI (20 mol%), Cs_2CO_3, $MeNH(CH_2)_2NHMe$, toluene, reflux; 72%. c) CF_3CO_2H, CH_2Cl_2; >85%. d) $Pd(OAc)_2$, CH_2Cl_2–MeOH, RT; 87%.

depicts the synthesis of two kinds of *meso*-phosphorylporphyrins. Copper-catalyzed C–P coupling of *meso*-iodoporphinatozinc **1Zn**[15] with di-*n*-butyl phosphite under Buchwald's conditions[16] afforded *meso*-(di-*n*-butoxyphosphoryl)-porphinatozinc **2Zn** in 81% yield (route a). Using diphenylphosphane oxide instead of di-*n*-butyl phosphite resulted in the formation of *meso*-diphenylphosphorylporphinatozinc **3Zn** in 72% yield (route b). In the latter reaction, a small amount of the phosphonic ester **4Zn** was obtained as a side product. Treatment of **2Zn**, **3Zn**, and **4Zn** with trifluoroacetic acid in CH_2Cl_2 afforded the corresponding free bases $\mathbf{2H_2}$, $\mathbf{3H_2}$, and $\mathbf{4H_2}$. Free base $\mathbf{3H_2}$ was then reacted with

$Pd(OAc)_2$ to give palladium phosphorylporphyrin **3Pd**. The structures of the newly synthesized porphyrins have been characterized by means of ^1H and ^{31}P NMR, UV/Vis absorption, IR absorption, and mass spectrometry.

The ^1H NMR spectra of phosphorylporphyrins $\mathbf{2H_2}$ and $\mathbf{3H_2}$ in $CDCl_3$ show distinct, sharp peaks for all of the protons (Figures S1 and S2 in the Supporting Information), with the signals of the peripheral β-protons at the 3- and 7-positions, the $POCH_2$ protons (for $\mathbf{2H_2}$), and the P-phenyl *ortho* protons (for $\mathbf{3H_2}$) being observed at $\delta = 10.24$ ($\mathbf{2H_2}$) or 9.42 ($\mathbf{3H_2}$), 4.13–4.46, and 7.94 ppm, respectively (for the numbering, see Figure 1). The palladium porphyrin (**3Pd**)

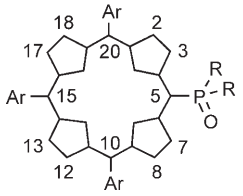

Figure 1. Numbering scheme of phosphorylporphyrins.

also exhibits well-resolved peaks, in almost the same regions as $\mathbf{3H_2}$. On the other hand, the ^1H NMR spectra of the zinc phosphorylporphyrins **2Zn** and **3Zn** in $CDCl_3$ or CD_2Cl_2 (ca. $(2–4)\times10^{-3}$ M) feature broad peaks at room temperature (Figures S3 and S4 in the Supporting Information). In particular, the protons adjacent to the P–oxo moieties of **2Zn** and **3Zn** are shielded and their signals are significantly broadened relative to the corresponding protons of $\mathbf{2H_2}$ and $\mathbf{3H_2}$. The broadening and upfield shifts are rather suppressed at higher temperatures (vide infra), suggesting that an equilibrium is set up between the zinc phosphorylporphyrin monomers and their aggregates. This is strongly supported by the UV/Vis absorption spectra of **2Zn** and **3Zn**, which show a concentration dependence in toluene (vide infra). Unfortunately, all attempts to measure the molecular weights of **2Zn** and **3Zn** in solution by vapor pressure osmometry have been unsuccessful owing to their limited solubility. However, the ESI mass spectra of **2Zn** and **3Zn** show parent ion peaks at m/z 2263 and 2278, respectively, attributable to the dimeric cations. These spectral data suggest that the **2Zn** and **3Zn** aggregates exist mostly as dimers in weakly polar solvents. In marked contrast, the ^1H NMR, UV/Vis absorption, and ESI mass spectra of $\mathbf{2H_2}$, $\mathbf{3H_2}$, and **3Pd** indicate that these phosphorylporphyrins exist as monomers.

When the ^1H NMR spectra of **2Zn** and **3Zn** were measured in $CD_3OD/CDCl_3$ (7:1 (v/v) for **2Zn**, 3:1 (v/v) for **3Zn**), the signals of the 3,7-β-, $POCH_2$-, and P-phenyl *ortho* protons were observed as sharp peaks at $\delta = 10.19$ (**2Zn**) or 9.22 (**3Zn**), 4.11–4.49, and 7.89 ppm, respectively (Figure S5 in the Supporting Information). These chemical shifts are close to those of the corresponding protons of $\mathbf{2H_2}$ and $\mathbf{3H_2}$, indicating that the aggregation of **2Zn** and **3Zn** is completely suppressed in the presence of methanol. The addition of an excess of pyridine to the solutions of **2Zn** and **3Zn** in $CDCl_3$ also shifted the equilibrium towards the monomer, with sharp resonances appearing due to the pyridine adducts **2Zn**·py and **3Zn**·py (Figure S6 in the Supporting Information). Based on these results, it can be concluded that the self-organization of **2Zn** and **3Zn** into the respective dimers is caused by coordination between the polarized P–oxo bond and the zinc center. In the presence of an excess of methanol or pyridine, the P–oxo–Zn coordination is disrupted by a competing P=O···H–OMe hydrogen-bonding interaction and/or E–Zn coordination (E = O, N). In contrast to **3Zn**, the phosphonic ester **4Zn** did not show aggregation behavior in solution. This indicates that the directional angle and distance of the P–oxo group from the porphyrin plane are important factors for the formation of a stable, complementary dimer in solution.

To gain further insight into the structures of the zinc–porphyrin dimers in solution, variable-temperature (VT) ^1H NMR measurements were carried out for **2Zn** and **3Zn**. Figure 2 depicts the temperature dependence of the spectra of **2Zn**. On increasing the temperature from 25 °C to 120 °C in $Cl_2CDCDCl_2$, the broad peaks due to the 2,8-β- and 3,7-β-protons gradually sharpen and shift downfield to $\delta = 9.0$ and 10.4 ppm, respectively. The spectrum observed at 120 °C is composed of one set of sharp peaks, characteristic of the **2Zn** monomer. On the other hand, on lowering the temperature from 20 °C to −50 °C in CD_2Cl_2, the broad peaks are split to give a second set of relatively sharp peaks, attributable to a symmetrically stacked **2Zn** dimer.[17] At −50 °C, the signals of the 2,8-β- and 3,7-β-protons appear at $\delta = 8.3$ and 7.4 ppm, respectively. It should be noted that the magnitudes of the upfield shifts of the signals of the peripheral β-protons on going from the monomer (at 120 °C) to the dimer (at −50 °C) increase in the order 13,17-β ($\Delta\delta \approx 0$ ppm) < 12,18-β (−0.05 ppm) < 2,8-β (−0.7 ppm) < 3,7-β (−3.0 ppm). The upfield shift of the signals of the β-protons distant from the phosphoryl group is negligible, whereas the upfield shift of the signals from the adjacent protons is significant.

A similar tendency was observed for **3Zn** (Figure S7 in the Supporting Information); the shifts in the signals of the peripheral β-protons on going from the monomer (in CD_3OD/CD_2Cl_2, 3:1 (v/v)) to the dimer (in CD_2Cl_2 at −60 °C) increase in the order 13,17-β ≈ 12,18-β ($\Delta\delta$ = +0.4 ppm) < 2,8-β (−0.9 ppm) < 3,7-β (−3.2 ppm). In addition, the signals of the P-phenyl protons also shift ($\Delta\delta$ = −0.6 ppm for *p*-H; −0.8 ppm for *m*-H; −3.4 ppm for *o*-H) as a result of dimerization. The remarkable upfield shifts observed for the protons adjacent to the phosphoryl groups are certainly due to the ring-current effect of the porphyrin π circuit, indicating that these moieties are located above the second porphyrin ring. Thus, it is most likely that the cofacial, partially overlapped zinc–porphyrin dimers are formed through P–oxo–Zn coordination, as illustrated in Equation (1) and Figure 3. This arrangement also explains the non-equivalence of the *ortho* protons of the 3,5-di-*tert*-butylphenyl groups at low temperatures. At −50 °C, the sig-

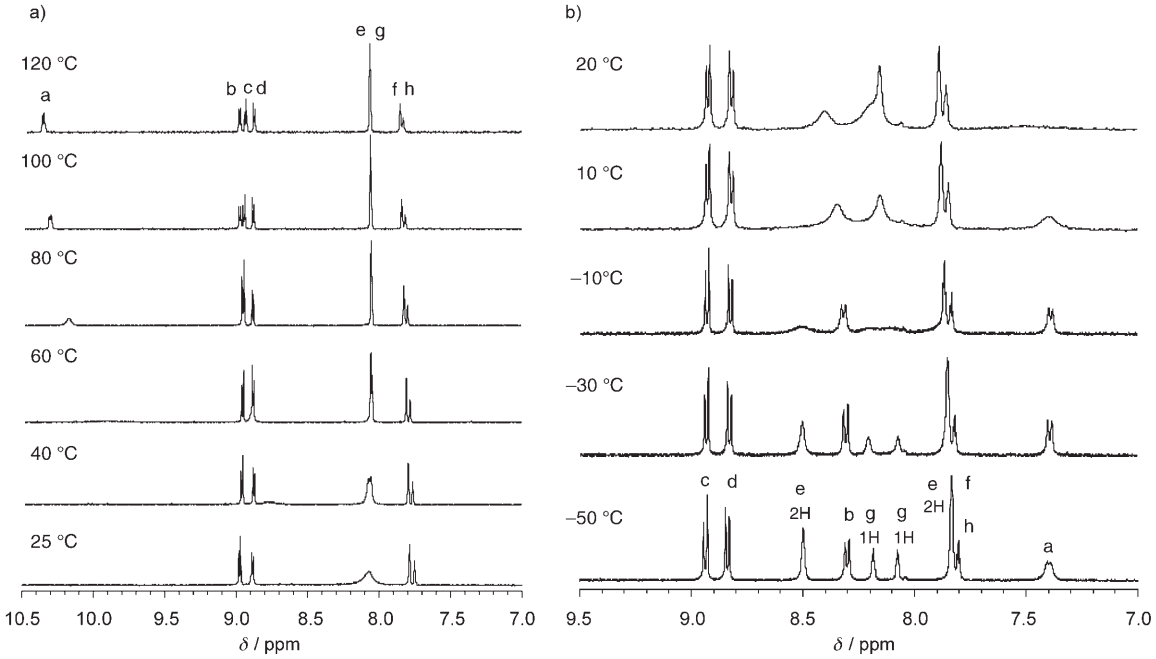

Figure 2. Temperature dependence of the ^{1}H NMR spectra of **2Zn** in chlorinated solvents. a) Measured in $Cl_2CDCDCl_2$ (2.0×10^{-3} M) from 25 °C to 120 °C at 400 MHz. b) Measured in CD_2Cl_2 (1.3×10^{-3} M) from 20 °C to −50 °C at 270 MHz. The labelled peaks are as follows: a = 3,7-β; b = 2,8-β; c = 12,18-β; d = 13,17-β; e = 10,20-H_o and -H_o'; f = 10,20-H_p; g = 15-H_o and -H_o'; h = 15-H_p. For the numbering, see Figure 1.

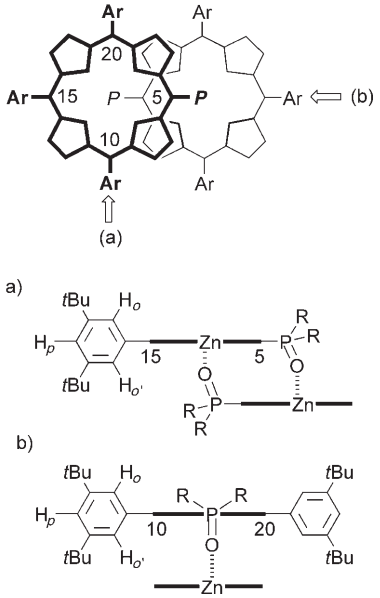

Figure 3. A model for the zinc *meso*-phosphorylporphyrin dimer. *P* = P(O)R_2; Ar = 3,5-di-*tert*-butylphenyl. a) Side view from the 10–20 axis. b) Side view from the 5–15 axis.

nals of the *ortho* protons of the 10- and 20-aryl groups and those of the 15-aryl group of **2Zn** are split into two resonances at δ = 7.84 and 8.50 ppm (each 2H) and δ = 8.07 and 8.19 ppm (each 1H), respectively. No such splitting for the *ortho* protons of free base $\mathbf{2H_2}$ is observed at −50 °C, suggesting that the inner and outer *ortho* protons of the complementary **2Zn** dimer are differentiated at this temperature.[18]

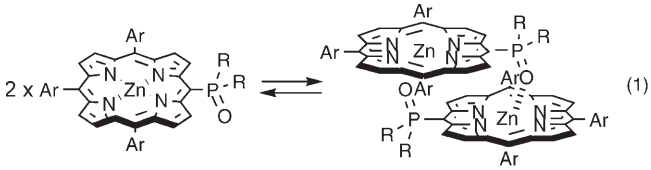

K_a (**2Zn**) = 1.4 x 10^4 M^{-1} (in toluene, at 25 °C)
K_a (**3Zn**) = 5.9 x 10^6 M^{-1} (in toluene, at 25 °C)

^{31}P NMR spectroscopy is a reliable tool for shedding light on the character of the phosphorus atom in a phosphoryl group. It has been reported that the ^{31}P peak of a cationic zinc–phosphane oxide complex, $[Zn(BF_4)_2(OPPh_3)_4]$ (δ = 42.9 ppm in $MeNO_2$),[19] appears significantly further downfield than that of free Ph_3PO (δ = 27 ppm), reflecting a deshielding of the P nucleus as a result of strong P–oxo–Zn coordination. However, the ^{31}P peak of **2Zn** was not seen to shift considerably in the range of −50 to +100 °C in VT-NMR measurements ($\Delta\delta_P \approx 2.5$ ppm at 2×10^{-3} M in $Cl_2CDCDCl_2$; $\Delta\delta_P \approx 1.0$ ppm at 2×10^{-3} M in [D_8]toluene). Thus, the ^{31}P chemical shifts of the zinc phosphorylporphyrin dimers differ only slightly from those of the monomers. This observation may be interpreted in terms of opposing shielding effects in the complementary dimers: the ring current from the facing porphyrin causes an upfield shift, whereas the P–oxo–Zn coordination causes a downfield shift. If these

effects are comparable, then the ^{31}P resonances will be affected only slightly by aggregation to the dimers.

Crystal structures of zinc phosphorylporphyrins: Single crystals of **2Zn** and **3Zn** were grown from hexane/$CHCl_3$ and MeCN/$CHCl_3$, respectively, and their structures were successfully elucidated by means of X-ray crystallography. As shown in Figure 4,[20] di-*n*-butoxyphosphorylporphinatozinc

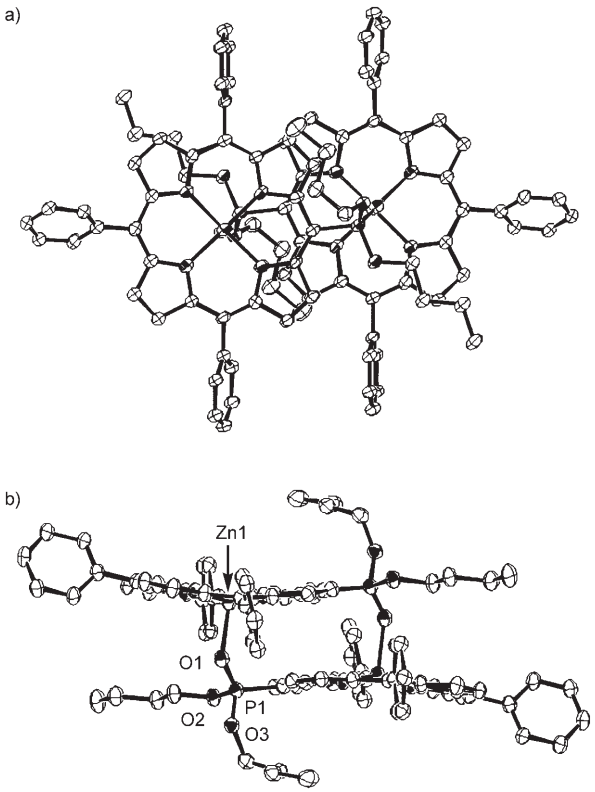

Figure 4. ORTEP diagrams of **2Zn** (30% probability ellipsoids). Hydrogen atoms and *tert*-butyl groups are omitted for clarity. a) Top view. b) Side view. Selected bond lengths [Å] and angles [°]: Zn1–O1 2.102(3), P1–O1 1.478(3), P1–O2 1.580(4), P1–O3 1.579(3); Zn1-O1-P1 133.4(2), O1-P1-O2 108.1(2), O1-P1-O3 111.9(2), O2-P1-O3 105.97(19).

2Zn exists as a cofacial, partially overlapped dimer connected through the complementary P–oxo–Zn coordination, in which the ester moiety and the pyrrole units adjacent to the phosphoryl group are located above the second porphyrin ring. The observed structural features are in good accordance with those deduced from the ^1H NMR spectra. Thus, the aggregation mode of the **2Zn** dimer in the solid state is probably close to that in solution. The Zn–O distance of 2.102(3) Å is longer than those observed for $ZnX_2(OPPh_3)_2$ (X = Cl, Br)[21] and $[Zn(BF_4)_2(OPPh_3)_4]$.[22] On the other hand, the P=O bond length of 1.478(3) Å is slightly longer than that in triphenylphosphane oxide (1.46 Å),[23] but shorter than the respective bond lengths of the aforementioned cationic Zn–$OPPh_3$ complexes. This indicates that the coordinative interaction between the P–oxo group and the zinc center in **2Zn** is weaker than those in $[ZnX_2(OPPh_3)_2]$ and $[Zn(BF_4)_2(OPPh_3)_4]$. Owing to this interaction, the five-coordinate zinc ion is displaced from the plane formed by the four nitrogen atoms (0.32 Å) and the porphyrin ring is distorted.

Schugar and co-workers have reported the crystal structures of the pyridine-tethered cofacial zinc–porphyrin dimers **5** (Figure 5).[2d] The porphyrin plane separations

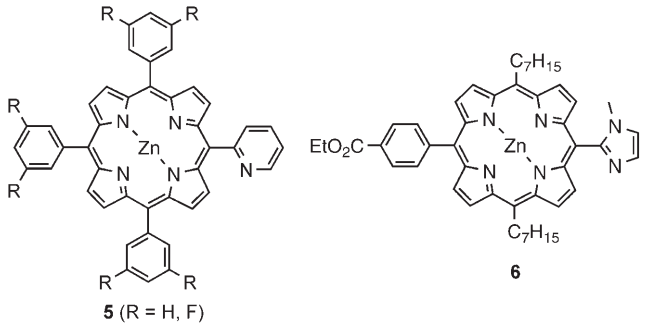

Figure 5. Structures of **5** and **6**.

around the phosphoryl groups in the **2Zn** dimer (3.3–3.4 Å) are close to the values reported for **5** (3.30–3.31 Å for the full 24 atoms). On the other hand, the Zn···Zn separation in the **2Zn** dimer (6.25 Å) is longer by about 0.3–0.4 Å relative to those in **5** (5.859(2)–5.955(2) Å). Furthermore, the displacement from the plane of the zinc atom in **2Zn** (0.32 Å) is smaller than those in **5** (0.39–0.40 Å), which suggests that the *meso*-2-pyridyl group coordinates to the zinc more strongly than the *meso*-di-*n*-butoxyphosphoryl group.

It is of interest that the observed structural features of the **2Zn** dimer resemble those of the chlorophyll pair in the primary electron donor, P700, of cyanobacterial photosystem I,[24] in which the chlorin planes are parallel at an interplanar distance of 3.6 Å and are partially overlapped with a center-to-center distance of 6.3 Å. The interaction between these chlorophyll rings is considered to be weak relative to that in purple bacterial reaction centers.[25] Therefore, the **2Zn** dimer may be regarded as a new model for such a weakly coupled chlorophyll pair in a photosynthetic reaction center.

In sharp contrast to **2Zn**, diphenylphosphorylporphinatozinc **3Zn** was found to exist as a linear polymeric structure as a result of unidirectional P–oxo–Zn coordination (Figure 6).[26] This aggregation mode differs markedly from that deduced from the ^1H NMR and mass spectra, which suggest that the complementary dimer is the prevalent species in solution. Such a difference in aggregation mode has been reported for 5-(4-pyridyl)-10,15,20-triphenylporphinatozinc, which is present as a linear polymeric structure in the solid state[2a] but exists mostly as a cyclic tetramer in solution.[27]

The mutual orientation of the porphyrin planes in **3Zn** is not parallel, as indicated by a mean dihedral angle between two neighboring porphyrin rings of 34.4°. On the other hand, the *meso*-C-P-O bond angle in **3Zn** (112.8(3)°) is

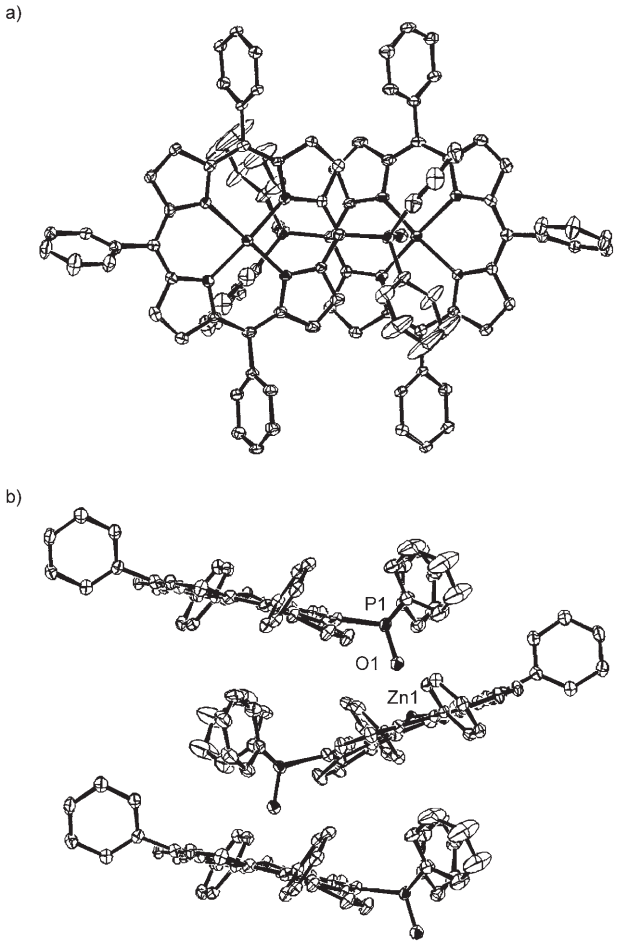

Figure 6. ORTEP diagrams of **3Zn** (30% probability ellipsoids). Hydrogen atoms and *tert*-butyl groups are omitted for clarity. Selected bond lengths [Å] and angles [°]: Zn1–O1 2.048(4), P1–O1 1.485(4); Zn1-O1-P1 176.7(3).

close to that in **2Zn** (114.2(2)°). As a result, the **3Zn** polymer has a much wider P-O-Zn angle (176.7(3)°) and a longer Zn···Zn distance (7.56 Å) relative to the **2Zn** dimer. The Zn–O distance (2.048(4) Å) in the **3Zn** polymer is slightly shorter than that in the **2Zn** dimer, while the P=O distance (1.485(4) Å) and the displacement of the zinc atom from the N_4 plane (0.32 Å) are comparable to those in **2Zn**. The difference in the packing modes between **2Zn** and **3Zn** may be ascribed to the different solvent systems employed for their recrystallization.[28] The observed structural features highlight another potential utility of the *meso*-phosphoryl group as a coordination site for the construction of linear zinc–porphyrin assemblies.

In the IR spectra of the solid samples, the P=O stretching bands of **2Zn** (ν = 1217 cm^{-1}) and **3Zn** (ν = 1180 cm^{-1}) are observed at lower frequencies than those of **$2H_2$** (ν = 1247 cm^{-1}) and **$3H_2$** (ν = 1187 cm^{-1}). These results imply that the multiple bond character of the P–oxo bond in the zinc phosphorylporphyrins is less than that in the corresponding free bases.

Optical properties of phosphorylporphyrins: As discussed above, in weakly polar solvents, **2Zn** and **3Zn** undergo self-organization at relatively high concentrations to form the corresponding complementary dimers. To ascertain the effects of aggregation on their optical properties, we measured the UV/Vis absorption spectra of these zinc phosphorylporphyrins under various conditions. In the absorption spectra of **3Zn** in toluene (2.5×10^{-7}–2.5×10^{-6} M), a splitting of the monomer Soret band was observed upon dimerization as a result of excitonic coupling (Figure 7).[29,30] The excitonic

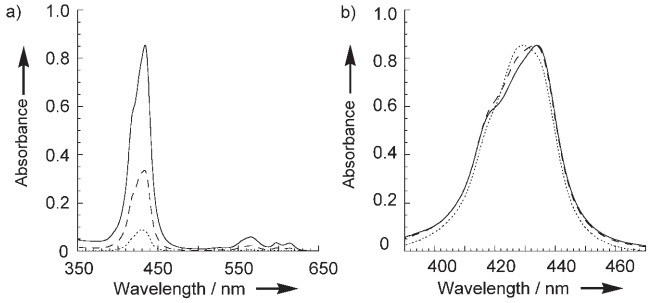

Figure 7. UV/Vis absorption spectra of **3Zn** in toluene at various concentrations: solid line, 2.5×10^{-6} M; dashed line, 1.0×10^{-6} M; dotted line, 2.5×10^{-7} M. a) 350–650 nm. b) 390–470 nm. The spectra in (b) are normalized for comparison.

band splitting was estimated by a curve-fitting analysis to be 940 cm^{-1},[31] which is comparable to the reported values for the pyridine-tethered porphyrin dimers **5** (ΔE = 900–1020 cm^{-1} for R = H, F).[2d] Porphyrin **2Zn** was only dimerized at much higher concentrations than **3Zn**, indicating that the binding ability of the phosphoryl group depends on the P substituents (vide infra). The splitting energy for **2Zn** could not be determined owing to the detection limit of its Soret band (Figure S8 in the Supporting Information). In marked contrast to those of the zinc phosphorylporphyrins, the UV/Vis absorption spectra of **$2H_2$**, **$3H_2$**, and **3Pd** did not show a concentration dependence, clearly indicating that these compounds exist as monomers in solution.

Adding an excess of pyridine or Ph_3PO to a solution of **2Zn** or **3Zn** caused a sharpening of the peaks in their UV/Vis absorption spectra due to the formation of N and O adducts of the zinc phosphorylporphyrin monomers (Figures S9 and S10 in the Supporting Information). The coordinating abilities of pyridine and Ph_3PO to the zinc centers were examined by titration experiments using 5,10,15,20-tetrakis(3,5-di-*tert*-butylphenyl)porphinatozinc (**7**) as a reference. The association constants for the pyridine and Ph_3PO adducts of **7** in toluene at 25 °C were determined as 1.9×10^3 and 6.3×10^2 M^{-1}, respectively [Eq. (2)].[32] Thus, the coordinating ability of Ph_3PO was found to be weaker than that of pyridine.

To examine the effect of the P substituents on the P–oxo–Zn coordination, the self-association constants (K_a) of **2Zn** and **3Zn** in toluene were determined by means of UV/Vis absorption competitive titration measurements. As listed

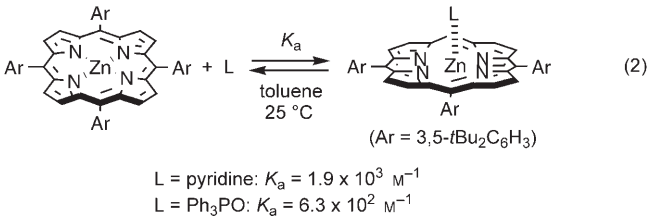

(2)

under Equation (1), the K_a value of **3Zn** ($5.9\times10^6\,\text{M}^{-1}$) is much larger than that of **2Zn** ($1.4\times10^4\,\text{M}^{-1}$), indicating that changing the P substituents can modify the coordinating abilities of phosphoryl ligands. It is also noteworthy that the K_a values of our *meso*-phosphorylporphyrins are significantly smaller than those of the *meso*-2-imidazolylporphyrins reported by Kobuke and co-workers.[33] Thus, the *meso*-phosphoryl groups bind to the porphyrin chromophores less tightly than the *meso*-imidazolyl groups, reflecting the difference in basicity of their lone pairs.

Photophysical and electrochemical properties of phosphorylporphyrins: To shed light on the effect of dimerization of the P–oxo-tethered porphyrins on their photophysical properties, we measured the fluorescence quantum yields and lifetimes of **2Zn** and **3Zn** under various conditions. The steady-state fluorescence spectra of **2Zn** and **3Zn** are depicted in Figure S11 in the Supporting Information. It was found that the fluorescence quantum yields of **2Zn** (ϕ_f = 0.059–0.060) and **3Zn** (ϕ_f = 0.040–0.042) vary only slightly in the concentration range of 1.0×10^{-4}–1.0×10^{-7} M in toluene. As shown in Figure S12 in the Supporting Information and Figure 8, the fluorescence lifetimes observed at higher concentrations (τ_f = 2.66 ns at 1.0×10^{-4} M for **2Zn**; τ_f = 1.88 ns at 6.9×10^{-6} M for **3Zn**) are almost the same as those observed at lower concentrations (τ_f = 2.69 ns at 3.4×10^{-7} M for **2Zn**; τ_f = 2.01 ns at 2.1×10^{-8} M for **3Zn**).[34] Moreover, the addition of an excess of Ph_3PO did not change the lifetime significantly (τ_f = 3.00 ns at 1.0×10^{-4} M for **2Zn** in the presence of 1000 equiv of Ph_3PO). These results imply that typical self-quenching from the S_1 states of **2Zn** and **3Zn** is negligible even in the dimeric states.

To investigate the effect of dimerization on the electrochemical properties, the oxidation potentials of **2Zn** and

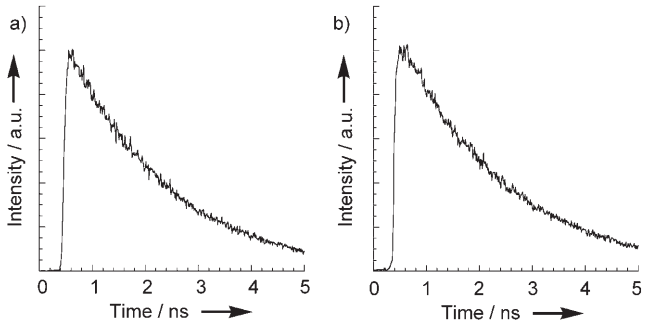

Figure 8. Fluorescence decay curves for **3Zn** in toluene, monitored at 620 nm (λ_{ex} = 420 nm). a) [**3Zn**] = 6.9×10^{-6} M: τ_f = 1.88 ns. b) [**3Zn**] = 2.1×10^{-8} M: τ_f = 2.01 ns.

3Zn were measured by means of cyclic voltammetry (CV) and differential pulse voltammetry (DPV) in CH_2Cl_2 at a concentration of 1.0×10^{-3} M, using nBu$_4$NPF$_6$ (TBAP) as an electrolyte (0.1 M). The voltammograms obtained for **3Zn** and **2Zn** are depicted in Figure 9 and in the Supporting Information (Figure S13), respectively. At this concentration, the zinc phosphorylporphyrins are considered to be present mainly in the dimeric state. The oxidation potentials [E_{ox} vs. Fc/Fc$^+$ (ne)] of **3Zn** were determined to be +0.29 (1e), +0.51 (1e), and +0.75 V (2e), where the number of electrons was approximated by comparison of the peak areas with those of the oxidation processes of TPP. The **2Zn** dimer gave rise to similar voltammograms with oxidation potentials of +0.35 (1e), +0.60 (1e), and +0.68 V (2e).

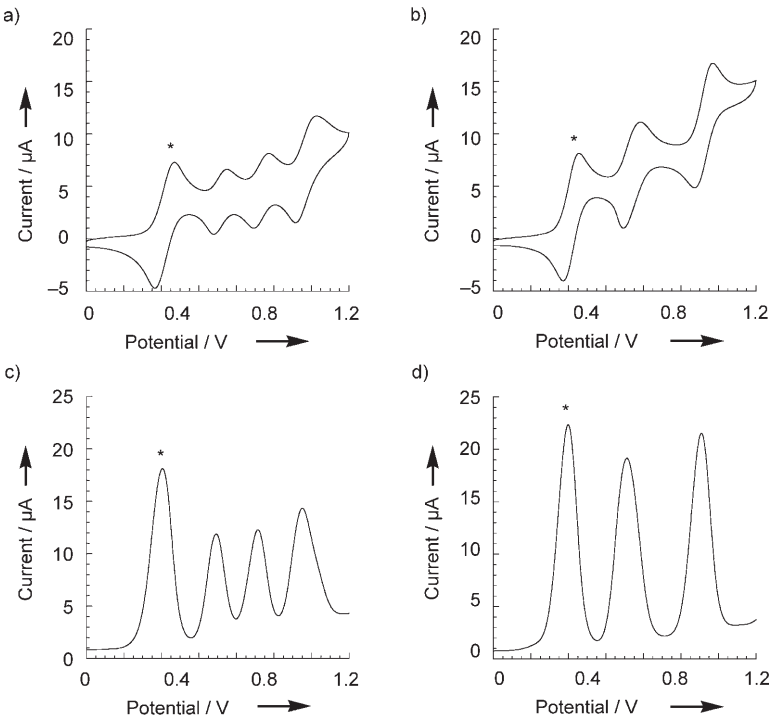

Figure 9. a), b) Cyclic voltammograms for **3Zn**. c), d) Differential pulse voltammograms for **3Zn**. Measured in CH_2Cl_2. [**3Zn**] = 1.0×10^{-3} M. [TBAP] = 0.1 M. Scan rate = 20 mV s^{-1}. Asterisks indicate the Fc/Fc$^+$ couple. a), c) In the absence of Ph_3PO. b), d) In the presence of Ph_3PO: [Ph_3PO] = 2.0×10^{-2} M.

Thus, the first oxidation processes of the zinc phosphorylporphyrin dimers are split into two reversible one-electron steps with a ΔE_{ox} of 0.25 V for **2Zn** and 0.22 V for **3Zn**. This type of 1 e/1 e/2 e electrochemical oxidation process has been observed for covalently linked cofacial porphyrin dimers, whereby the differences in the first two steps (ΔE_{ox}) were reported to be 0.07–0.31 V.[35] It therefore seems likely that there is efficient delocalization of the radical cation over the two porphyrin rings in the **2Zn** and **3Zn** dimers. On the other hand, the second oxidation process occurs by a reversible two-electron step, implying that there remains a very weak interaction between the porphyrin chromophores in the π-cation radical dimers. When an excess of Ph_3PO was added to the solution, the voltammograms of **2Zn** and **3Zn** changed dramatically. The Ph_3PO adducts of the zinc phosphorylporphyrin monomers were oxidized in two reversible one-electron processes with E_{ox} values of +0.33 (1 e) and +0.74 V (1 e) for **2Zn** and +0.32 (1 e) and +0.71 V (1 e) for **3Zn**.

It should be noted here that the electrochemical properties observed for the P–oxo-tethered zinc–porphyrin dimers differ considerably from those reported for pyridine- and imidazole-tethered zinc–porphyrin dimers. In these N-tethered systems, both the first and second oxidation processes occur by two reversible one-electron steps: Schugar's dimer **5** shows four separate one-electron oxidation potentials at +0.56, +1.01, +1.21, and +1.55 V (vs. SCE; in CH_2Cl_2 containing nBu$_4$NBF$_4$),[36] and Kobuke's dimer **6** exhibits oxidation potentials at +0.414, +0.632, +0.968, and +1.120 V (vs. Ag/Ag$^+$; in $CHCl_3$ containing TBAP).[3f] Interestingly, the phosphoryl linkers examined here are not capable of connecting the porphyrin radical cations so as to influence their HOMO energies, whereas the N-heterocyclic linkers affect them strongly.

Conclusion

We have established a general and straightforward method for the synthesis of *meso*-phosphorylporphyrins, and have elucidated their crystal structures, photophysical properties, and electrochemical properties for the first time. The observed aggregation behavior of the zinc phosphorylporphyrins strongly depends on the P substituents and the presence of additives. It has also been found that the coordinating abilities of the peripheral phosphoryl ligands differ considerably from those of N-heterocyclic ligands. The photophysical and electrochemical properties of the P–oxo-tethered complementary porphyrin dimers demonstrate their potential utilities as new structural models for investigating the energy- and electron-transfer processes occurring at a photosynthetic reaction center with a weakly coupled special pair.

Experimental Section

General: ^{1}H and ^{31}P NMR spectra were measured on a JEOL EX400 spectrometer. Chemical shifts are reported as relative values versus tetramethylsilane (^{1}H) and H_3PO_4 (^{31}P), respectively. Matrix-assisted laser desorption/ionization (MALDI) time-of-flight (TOF) mass spectra and ESI mass spectra were measured on a Shimadzu Kratos Compact MALDI I spectrometer and an Applied Biosystems Mariner biospectrometry workstation, respectively. FAB mass spectra were measured on a JEOL JMS-HS110 spectrometer using 3-nitrobenzyl alcohol as a matrix. IR spectra were recorded from samples in KBr pellets on a Shimadzu FTIR-8200A spectrophotometer. UV/Vis absorption spectra were obtained on a Perkin Elmer Lambda 900 UV/Vis/NIR spectrophotometer. Electrochemical measurements were performed on a CH Instruments model 660A electrochemical workstation using a glassy carbon working electrode, a platinum wire counter electrode, and an Ag/Ag$^+$ [0.01 M $AgNO_3$, 0.1 M nBu$_4$NPF$_6$ (MeCN)] reference electrode. The potentials were calibrated with ferrocenium/ferrocene [E_{mid} = +0.20 V vs. Ag/Ag$^+$]. Steady-state fluorescence spectra were measured on a Fluorolog 3 spectrofluorimeter (ISA Inc.) equipped with a cooled IR-sensitive photomultiplier (R2658). Time-resolved fluorescence measurements were performed by using a single-photon counting method based on second harmonic generation (SHG, 400 nm) of a Ti-sapphire laser (Spectra-Physics, Tsunami 3950 L2S, FWHM 100 fs) pumped with a diode-pumped solid-state laser (Spectra-Physics, Millennia VIs, 6.0 W) as excitation source and a streakscope (Hamamatsu Photonics, C4334–01) equipped with a polychromator (Acton Research, SpectraPro 150) as detector. Lifetimes were evaluated with the software supplied with the equipment. Dichloromethane (CH_2Cl_2) and toluene were distilled from CaH_2 before use. 5-Iodo-10,15,20-tris(3,5-di-*tert*-butylphenyl)porphinatozinc (**1Zn**) was prepared according to the reported procedure.[15] Other chemicals and solvents were of reagent grade quality, purchased commercially, and used without further purification unless otherwise noted. Thin-layer chromatography and flash column chromatography were performed with Art 5554 DC-Alufolien Kieselgel 60 F_{254} (Merck) and silica gel 60N (Kanto Chemicals), respectively. All reactions were performed under an argon atmosphere unless otherwise stated.

5-Di-*n*-butoxyphosphoryl-10,15,20-tris(3,5-di-*tert*-butylphenyl)porphinatozinc(II) (2Zn): A 30 mL flask containing **1Zn** (200 mg, 0.188 mmol), CuI (15 mg, 0.039 mmol), and Cs_2CO_3 (660 mg, 2.03 mmol) was evacuated in vacuo and then filled with argon. The same manipulation was carried out three times. Toluene (10 mL), *N*,*N*′-dimethylethylenediamine (30 μL, 0.28 mmol), and di-*n*-butyl phosphite (60 μL, 0.31 mmol) were added to the reaction mixture by means of syringes, and the resulting mixture was stirred at 130 °C. After 6–7 h, the **1Zn** had been completely consumed (as shown by TLC analysis). The mixture was then filtered through a bed of Celite, and the filtrate was concentrated under reduced pressure to leave a solid, which was subjected to chromatography on silica gel using hexane and CH_2Cl_2 as eluents. The reddish-purple fraction ($R_f \approx 0.3$ in hexane/CH_2Cl_2, 20:80) was collected, concentrated, and recrystallized from CH_2Cl_2/MeOH to give **2Zn** (171 mg, 81 %). ^{1}H NMR ($CDCl_3$, 4.4 mM): δ = 0.61 (br, 6H; CH_2CH_3), 0.8–1.4 (br, 8H; $OCH_2CH_2CH_2CH_3$), 1.52 (s, 18H; $C(CH_3)_3$), 1.55 (s, 36H; $C(CH_3)_3$), 3.10–3.60 (br, 4H; OCH_2CH_2), 7.78 (t, 1H, J = 1.8 Hz; *p*-Ar-H), 7.82 (t, 2H, J = 1.8 Hz; *p*-Ar-H), 8.07 (d, 2H, J = 1.8 Hz; *o*-Ar-H), 8.12 (d, 4H, J = 1.8 Hz; *o*-Ar-H), 8.77 (br, 2H; β-H), 8.86 (d, 2H, J = 4.4 Hz; β-H), 8.94 (d, 2H, J = 4.4 Hz; β-H), 8.8–9.2 ppm (br, 2H; β-H); ^{1}H NMR ($CD_3OD/CDCl_3$, 7:1 (v/v), 2.6 mM): δ = 0.84 (t, 6H, J = 7.3 Hz; CH_2CH_3), 1.42–1.56 (m, 4H; CH_2CH_3), 1.55 (s, 18H; $C(CH_3)_3$), 1.57 (s, 36H; $C(CH_3)_3$), 1.68–1.76 (m, 4H; OCH_2CH_2), 4.11–4.22 (m, 2H; OCH_2CH_2), 4.38–4.49 (m, 2H; OCH_2CH_2), 7.86 (s, 1H; *p*-Ar-H), 7.88 (s, 2H; *p*-Ar-H), 8.07 (s, 6H; *o*-Ar-H), 8.74 (d, 2H, J = 4.8 Hz; β-H), 8.81 (d, 2H, J = 4.8 Hz; β-H), 8.88 (d, 2H, J = 4.8 Hz; β-H), 10.19 ppm (d, 2H, J = 4.8 Hz; β-H); ^{31}P NMR ($CDCl_3$, 4.4 mM): δ = 22.4 ppm; ^{31}P NMR ($CD_3OD/CDCl_3$, 7:1 (v/v), 2.6 mM): δ = 24.4 ppm; ^{31}P NMR ([D_8]toluene; 4 mM): δ = 22.5 ppm; MS (ESI): m/z: 1129.6 ([M+H]$^+$, 85), 2263.2 ([2M+3H]$^+$, 100); IR (KBr): $\tilde{\nu}$ = 1217 cm^{-1} (P=O); UV/Vis

(toluene, 5.0×10^{-6} M): λ_{max} (ε) = 423 (438000), 550 (18400), 583 nm (8900 $M^{-1}cm^{-1}$).

5-Di-*n*-butoxyphosphoryl-10,15,20-tris(3,5-di-*tert*-butylphenyl)porphine ($2H_2$): Trifluoroacetic acid (0.12 mL) was added to a solution of **2Zn** (75 mg, 0.066 mmol) in CH_2Cl_2 (15 mL), and the resulting mixture was stirred at room temperature for 3 h. After checking the consumption of **2Zn** by TLC, the mixture was poured into water (15 mL). The organic phase was separated, and the aqueous phase was twice extracted with CH_2Cl_2. The combined organic extracts were washed with aqueous $NaHCO_3$ and water, dried over Na_2SO_4, and concentrated under reduced pressure to leave a solid, which was recrystallized from CH_2Cl_2/MeOH to give **$2H_2$** (60 mg, 85%). ^{1}H NMR ($CDCl_3$): δ = −2.20 (s, 2H; NH), 0.80 (t, 6H, J = 7.3 Hz; CH_2CH_3), 1.37–1.54 (m, 4H; CH_2CH_3), 1.51 (s, 18H; $C(CH_3)_3$), 1.53 (s, 36H; $C(CH_3)_3$), 1.64–1.76 (m, 4H; OCH_2CH_2), 4.13 (ddt, 2H, J = 9.9, 6.6, 6.6 Hz; OCH_2CH_2), 4.46 (ddt, 2H, J = 9.9, 6.6, 6.6 Hz; OCH_2CH_2), 7.78 (t, 1H, J = 1.8 Hz; p-Ar-H), 7.81 (t, 2H, J = 1.8 Hz; p-Ar-H; OCH_2CH_3), 8.02 (d, 2H, J = 1.8 Hz; o-Ar-H), 8.04 (d, 4H, J = 1.8 Hz; o-Ar-H), 8.75 (d, 2H, J = 4.8 Hz; β-H), 8.83 (d, 2H, J = 4.8 Hz; β-H), 8.90 (d, 2H, J = 4.8 Hz; β-H), 10.24 ppm (d, 2H, J = 4.8 Hz; β-H); ^{31}P NMR ($CDCl_3$): δ = 20.8 ppm; MS (ESI): m/z = 1067.7 ($[M+H]^+$); IR (KBr): $\tilde{\nu}$ = 1247 cm^{-1} (P=O); UV/Vis (toluene): λ_{max} (ε) = 420 (351000), 516 (17600), 551 (9400), 589 (6300), 643 nm (4300 $M^{-1}cm^{-1}$).

5-Diphenylphosphoryl-10,15,20-tris(3,5-di-*tert*-butylphenyl)porphinatozinc(II) (3Zn): This compound was prepared from **1Zn** and diphenylphosphane oxide according to a similar procedure to that described for the synthesis of **2Zn**. A reddish-purple fraction ($R_f \approx 0.74$ in CH_2Cl_2/acetone, 95:5) was collected by column chromatography on silica gel, concentrated, and recrystallized from CH_2Cl_2/MeOH to give **3Zn** and **4Zn** in yields of 72% and 5%, respectively. **3Zn**: ^{1}H NMR ($CD_3OD/CDCl_3$, 3:1 (v/v)): δ = 1.51 (s, 36H; CH_3), 1.54 (s, 18H; CH_3), 7.49 (dt, 4H, J = 3.0, 7.3 Hz; m-Ph), 7.60 (t, 2H, J = 7.3 Hz; p-Ph), 7.78 (t, 1H, J = 2.0 Hz; p-Ar-H), 7.82 (t, 2H, J = 2.0 Hz; p-Ar-H), 7.89 (dd, 4H, J = 12.2, 7.3 Hz; o-Ph), 7.97 (d, 2H, J = 2.0 Hz; o-Ar-H), 8.06 (d, 4H, J = 2.0 Hz; o-Ar-H), 8.58 (d, 2H, J = 4.9 Hz; β-H), 8.73 (d, 2H, J = 4.4 Hz; β-H), 8.82 (d, 2H, J = 4.4 Hz; β-H), 9.22 ppm (d, 2H, J = 4.9 Hz; β-H); ^{31}P NMR ($CDCl_3$): δ = 25.0 ppm; ^{31}P NMR ($CD_3OD/CDCl_3$, 3:1 (v/v)): δ = 36.1 ppm; IR (KBr): $\tilde{\nu}$ = 1180 cm^{-1} (P=O); UV/Vis (toluene, 1.7×10^{-7} M): λ_{max} (ε) = 428 (204000), 563 (19200), 615 nm (12400 $M^{-1}cm^{-1}$); MS (ESI): m/z: 1138.54 ($[M+H]^+$, 88), 2278.13 ($[2M+2H]^+$, 100). **4Zn**: ^{1}H NMR ($CDCl_3$): δ = 1.51 (s, 36H; CH_3), 1.54 (s, 18H; CH_3), 7.50 (m, 4H; m-Ph), 7.58 (m, 2H; p-Ph), 7.76 (s, 3H; Ar-H), 8.01 (s, 4H; o-Ar-H), 8.03 (s, 2H; p-Ar-H), 8.03 (m, 4H; o-Ph), 8.80 (d, 2H, J = 4.4 Hz; β-H), 8.94 (s, 4H; β-H), 9.18 ppm (s, 2H; β-H); ^{31}P NMR ($CDCl_3$): δ = 32.0 ppm; UV/Vis (toluene): λ_{max} (ε) = 424 (483000), 552 (17300), 593 nm (5500 $mol^{-1}m^3cm^{-1}$); MS (MALDI-TOF): m/z = 1156 ($[M+H]^+$, 100).

5-Diphenylphosphoryl-10,15,20-tris(3,5-di-*tert*-butylphenyl)porphine ($3H_2$): This compound was prepared from **3Zn** and trifluoroacetic acid according to the procedure described for the synthesis of **$2H_2$**. ^{1}H NMR ($CDCl_3$): δ = −1.98 (s, 2H; NH), 1.49 (s, 36H; CH_3), 1.51 (s, 18H; CH_3), 7.43 (m, 4H; m-Ph), 7.53 (t, 2H, J = 7.6 Hz; p-Ph), 7.75 (s, 2H; p-Ar-H), 7.78 (s, 1H; p-Ar-H), 7.94 (m, 4H; o-Ph), 7.97 (s, 4H; o-Ar-H), 8.02 (s, 2H; o-Ar-H), 8.62 (d, 2H, J = 4.8 Hz; β-H), 8.73 (d, 2H, J = 4.8 Hz; β-H), 8.82 (d, 2H, J = 4.8 Hz; β-H), 9.42 ppm (br, 2H; β-H); ^{31}P NMR ($CDCl_3$): δ = 31.6 ppm; MS (FAB): m/z: 1075.7 ($[M+H]^+$, 100); MS (ESI): m/z: 1075.64 ($[M+H]^+$, 100); IR (KBr): $\tilde{\nu}$ = 1187 cm^{-1} (P=O); UV/Vis (toluene): λ_{max} (ε) = 425 (260000), 521 (13400), 557 (7700), 593 (5100), 647 nm (3700 $M^{-1}cm^{-1}$).

5-Diphenylphosphoryl-10,15,20-tris(3,5-di-*tert*-butylphenyl)porphinatopalladium(II) (3Pd): A mixture of **$3H_2$** (35.5 mg, 0.0330 mmol), $Pd(OAc)_2$ (16.0 mg, 0.0712 mmol), CH_2Cl_2 (15 mL), and CH_3OH (15 mL) was stirred overnight at room temperature in the dark. The solvent was then removed and the residue was repeatedly extracted with CH_2Cl_2. The combined organic extracts were washed with 3% aqueous $NaHCO_3$ and water, dried over Na_2SO_4, and concentrated under reduced pressure to leave a solid, which was recrystallized from CH_2Cl_2/MeOH to give **3Pd** (33.8 mg, 0.0286 mmol, 86.7%). ^{1}H NMR (400 MHz, $CDCl_3$): δ = 1.48 (s, 36H; CH_3), 1.50 (s, 18H; CH_3), 7.43 (m, 4H; m-Ph), 7.54 (m, 2H; p-Ph), 7.74 (t, 2H, J = 2.0 Hz; p-Ar-H), 7.77 (t, 1H, J = 1.5 Hz; p-Ar-H), 7.90 (m, 4H; o-Ph), 7.93 (d, 4H, J = 2.0 Hz; o-Ar-H), 7.97 (d, 2H, J = 1.5 Hz; o-Ar-H), 8.65 (d, 2H, J = 4.8 Hz; β-H), 8.75 (d, 2H, J = 4.8 Hz; β-H), 8.81 (d, 2H, J = 4.8 Hz; β-H), 9.46 ppm (d, 2H, J = 4.8 Hz; β-H); ^{31}P NMR ($CDCl_3$): δ = 31.5 ppm; MS (MALDI-TOF): m/z : 1179.0 ($[M+H]^+$, 100); UV/Vis (toluene): λ_{max} (ε) = 421 (279000), 531 (14700), 565 nm (10100 $M^{-1}cm^{-1}$).

5-Diphenylphosphoxyl-10,15,20-tris(3,5-di-*tert*-butylphenyl)porphine ($4H_2$): This compound was prepared from **4Zn** and trifluoroacetic acid according to the procedure described for the synthesis of **$2H_2$**. ^{1}H NMR ($CDCl_3$): δ = −2.77 (s, 2H; NH), 1.50 (s, 36H; CH_3), 1.55 (s, 18H; CH_3), 7.47 (m, 4H; m-Ph), 7.56 (m, 2H; p-Ph), 7.76 (s, 2H; p-Ar-H), 7.77 (s, 1H; p-Ar-H), 8.01 (s, 6H; o-Ar-H), 8.11 (m, 4H; o-Ph), 8.72 (d, 2H, J = 4.8 Hz; β-H), 8.82 (d, 2H, J = 4.8 Hz; β-H), 8.83 (d, 2H, J = 4.8 Hz; β-H), 9.25 ppm (d, 2H, J = 4.4 Hz; β-H); ^{31}P NMR ($CDCl_3$): δ = 32.4 ppm; MS (MALDI-TOF): m/z: 1092 ($[M+H]^+$, 100); UV/Vis (toluene): λ_{max} (ε) = 420 (439000), 517 (16500), 552 (11400), 595 (5200), 652 nm (6500 $M^{-1}cm^{-1}$). The structure of **$4H_2$** was confirmed by X-ray diffraction analysis, although the quality of the crystallographic data was considered insufficient to permit discussion of the bond parameters.

Determination of association constants: The association constants of the **2Zn** and **3Zn** dimers [given below Eq. (1)] and the **7**·pyridine and **7**·Ph_3PO adducts [given below Eq. (2)] were determined by competitive UV/Vis absorption measurements at 25°C using SPECFIT. Selected results are depicted in Figures S9 and S10 in the Supporting Information.

X-ray crystallographic analyses

*Porphyrin **2Zn***: Intensity data were collected on a Rigaku RAXIS-RAPID imaging plate area detector using graphite-monochromated $Cu_{K\alpha}$ radiation (λ = 1.54178 Å). The data were corrected for Lorentz and polarization effects. The structures were solved by direct methods[37] and expanded using Fourier techniques.[38] Non-hydrogen atoms were refined anisotropically. Hydrogen atoms were refined as a riding model. All calculations were performed using the CrystalStructure[39,40] crystallographic software package, except for the refinement, which was performed using SHELXL-97.[41]

*Porphyrin **3Zn***: The intensity data were collected on a RIGAKU Saturn 70 CCD system equipped with a VariMax Mo Optic set-up using $Mo_{K\alpha}$ radiation (λ = 0.71070 Å). The structures were solved by direct methods (SHELXS-97) and refined by full-matrix least-squares procedures on F^2 for all reflections (SHELXL-97).[41] All hydrogen atoms of **1** were positioned using AFIX instructions, while the hydrogen atoms of H_2O were placed in reasonable positions using DFIX constructions and were refined isotropically. All other atoms were refined anisotropically.

Acknowledgements

This work was partially supported by Grants-in-Aid (No. 17350018, and 21st Century COE on Kyoto University Alliance for Chemistry) from the Ministry of Education, Culture, Sports, Science and Technology of Japan. H.I. also thanks the Sekisui and Kurata foundations for financial support. We thank Dr. Koji Sasaki for his assistance with the ESI mass measurements and Dr. Yutaka Hitomi for his assistance with the calculation of association constants.

[1] a) J. K. M. Sanders in *Comprehensive Supramolecular Chemistry Vol. 9* (Eds.: J. Atwood, E. Davies, D. MacNicol, F. Vögtle, J.-M. Lehn), Pergamon Press, Oxford, **1996**, pp. 131–164; b) V. Balzani, F. Scandola in *Comprehensive Supramolecular Chemistry Vol. 10* (Eds.: J. Atwood, E. Davies, D. MacNicol, F. Vögtle, J.-M. Lehn), Pergamon Press, Oxford, **1996**, pp. 687–764; c) J. K. M. Sanders in *The Porphyrin Handbook Vol. 3* (Eds.: K. M. Kadish, K. M. Smith, R. Guilard), Academic Press, San Diego, **2000**, pp. 347–368; d) J.-C. Chambron, V. Heitz, J.-P. Sauvage in *The Porphyrin Handbook Vol. 6* (Eds.: K. M. Kadish, K. M. Smith, R. Guilard), Academic

Press, San Diego, **2000**, pp. 1–42; e) T. Imamura, K. Fukushima, *Coord. Chem. Rev.* **2000**, *198*, 133; f) J. Wojaczynski, L. Latos-Grazynski, *Coord. Chem. Rev.* **2000**, *204*, 113; g) L. Baldini, C. A. Hunter, *Adv. Inorg. Chem.* **2002**, *53*, 213; h) E. Iengo, E. Zangrando, E. Alessio, *Eur. J. Inorg. Chem.* **2003**, 2371; i) P. D. Harvey in *The Porphyrin Handbook Vol. 18* (Eds.: K. M. Kadish, K. M. Smith, R. Guilard), Academic Press, San Diego, **2003**, pp. 63–250; j) Y. Kobuke, *J. Porphyrins Phthalocyanines* **2004**, *8*, 156; k) C. M. Drain, I. Goldberg, I. Sylvain, A. Falber, *Top. Curr. Chem.* **2005**, *245*, 55; l) A. Satake, Y. Kobuke, *Tetrahedron* **2005**, *61*, 13; m) T. S. Balaban, *Acc. Chem. Res.* **2005**, *38*, 612, and references therein.

[2] For example, see: a) E. B. Fleischer, A. M. Shachter, *Inorg. Chem.* **1991**, *30*, 3763; b) C. A. Hunter, L. D. Sarson, *Angew. Chem.* **1994**, *106*, 2424; *Angew. Chem. Int. Ed. Engl.* **1994**, *33*, 2313; c) C. M. Drain, J.-M. Lehn, *J. Chem. Soc. Chem. Commun.* **1994**, 2313; d) R. T. Stibrany, J. Vasudevan, S. Knapp, J. A. Potenza, T. Emge, H. J. Schugar, *J. Am. Chem. Soc.* **1996**, *118*, 3980; e) L. D. Sarson, K. Ueda, M. Takeuchi, S. Shinkai, *Chem. Commun.* **1996**, 619; f) R. V. Slone, J. T. Hupp, *Inorg. Chem.* **1997**, *36*, 5422; g) K. Funatsu, T. Imamura, A. Ichimura, Y. Sasaki, *Inorg. Chem.* **1998**, *37*, 4986; h) J. Fan, J. A. Whiteford, B. Olenyuk, M. D. Levin, P. J. Stang, E. B. Fleischer, *J. Am. Chem. Soc.* **1999**, *121*, 2741; i) A. Prodi, M. T. Indelli, C. J. Kleverlaan, F. Scandola, E. Alessio, T. Gianferrara, L. G. Marzilli, *Chem. Eur. J.* **1999**, *5*, 2668; j) S. L. Darling, C. C. Mak, N. Bampos, N. Feeder, S. J. Teat, J. K. M. Sanders, *New J. Chem.* **1999**, *23*, 359; k) D. Sun, F. S. Tham, C. A. Reed, L. Chaker, M. Burgess, P. D. W. Boyd, *J. Am. Chem. Soc.* **2000**, *122*, 10704; l) A. Tsuda, T. Nakamura, S. Sakamoto, K. Yamaguchi, A. Osuka, *Angew. Chem.* **2002**, *114*, 2941; *Angew. Chem. Int. Ed.* **2002**, *41*, 2817; m) E. Iengo, E. Zangrando, S. Geremia, R. Graff, B. Kieffer, E. Alessio, *Chem. Eur. J.* **2002**, *8*, 4670; n) A. Tsuda, S. Sakamoto, K. Yamaguchi, T. Aida, *J. Am. Chem. Soc.* **2003**, *125*, 15722; o) M. Vinodu, Z. Stein, I. Goldberg, *Inorg. Chem.* **2004**, *43*, 7582.

[3] For example, see: a) Y. Kobuke, H. Miyaji, *J. Am. Chem. Soc.* **1994**, *116*, 4111; b) Y. Kobuke, H. Miyaji, *Bull. Chem. Soc. Jpn.* **1996**, *69*, 3563; c) K. Ogawa, Y. Kobuke, *Angew. Chem.* **2000**, *112*, 4236; *Angew. Chem. Int. Ed.* **2000**, *39*, 4070; d) Y. Kobuke, K. Ogawa, *Bull. Chem. Soc. Jpn.* **2003**, *76*, 689; e) R. Takahashi, Y. Kobuke, *J. Am. Chem. Soc.* **2003**, *125*, 2372; f) H. Ozeki, A. Nomoto, K. Ogawa, Y. Kobuke, M. Murakami, K. Hosoda, M. Ohtani, S. Nakashima, H. Miyasaka, T. Okada, *Chem. Eur. J.* **2004**, *10*, 6393.

[4] T. S. Balaban, R. Goddard, M. Linke-Schaetzel, J.-M. Lehn, *J. Am. Chem. Soc.* **2003**, *125*, 4233.

[5] For example, see: a) J. Mårtensson, K. Sandros, O. Wennerström, *Tetrahedron Lett.* **1993**, *34*, 541; b) S. Knapp, J. Vasudevan, T. J. Emge, B. H. Arison, J. A. Potenza, H. J. Schugar, *Angew. Chem.* **1998**, *110*, 2537; *Angew. Chem. Int. Ed.* **1998**, *37*, 2368; c) M. Gardner, A. J. Guerin, C. A. Hunter, U. Michelsen, C. Rotger, *New J. Chem.* **1999**, *23*, 309.

[6] a) T. S. Balaban, A. D. Bhise, M. Fischer, M. Linke-Schaetzel, C. Roussel, N. Vanthuyne, *Angew. Chem.* **2003**, *115*, 2189; *Angew. Chem. Int. Ed.* **2003**, *42*, 2140; b) H. Tamiaki, S. Kimura, T. Kimura, *Tetrahedron* **2003**, *59*, 7423; c) T. S. Balaban, M. Linke-Schaetzel, A. D. Bhise, N. Vanthuyne, C. Roussel, *Eur. J. Org. Chem.* **2004**, 3919; d) T. S. Balaban, M. Linke-Schaetzel, A. D. Bhise, N. Vanthuyne, C. Roussel, C. E. Anson, G. Buth, A. Eichhöfer, K. Foster, G. Garab, H. Gliemann, R. Goddard, T. Javorfi, A. K. Powell, H. Rösner, T. Schimmel, *Chem. Eur. J.* **2005**, *11*, 2267.

[7] a) H. Tamiaki, A. R. Holzwarth, K. Schaffner, *J. Photochem. Photobiol. B* **1992**, *15*, 355; b) H. Tamiaki, M. Amakawa, A. R. Holzwarth, K. Schaffner, *Photosynth. Res.* **2002**, *71*, 59; c) V. Huber, M. Katterle, M. Lysetska, F. Würthner, *Angew. Chem.* **2005**, *117*, 3208; *Angew. Chem. Int. Ed.* **2005**, *44*, 3147; d) M. Kunieda, H. Tamiaki, *Eur. J. Org. Chem.* **2006**, 2352; e) C. Röger, M. G. Müller, M. Lysetska, Y. Miloslavina, A. R. Holzwarth, F. Würthner, *J. Am. Chem. Soc.* **2006**, *128*, 6542.

[8] For anionic phenoxy and hydroxy ligands, see: a) H. M. Goff, E. T. Shimomura, Y. J. Lee, W. R. Scheidt, *Inorg. Chem.* **1984**, *23*, 315; b) G. M. Godziela, D. Tilotta, H. M. Goff, *Inorg. Chem.* **1986**, *25*, 2142; c) J. Wojaczyński, L. Latos-Grażyński, *Inorg. Chem.* **1995**, *34*, 1054; d) A. L. Balch, L. Latos-Grażyński, T. N. St. Claire, *Inorg. Chem.* **1995**, *34*, 1395; e) J. Wojaczynski, L. Latos-Grażyński, *Inorg. Chem.* **1996**, *35*, 4812.

[9] a) S. L. Darling, E. Stulz, N. Feeder, N. Bampos, J. K. M. Sanders, *New J. Chem.* **2000**, *24*, 261; b) E. Stulz, M. Maue, N. Feeder, S. J. Teat, Y.-F. Ng, A. D. Bond, S. L. Darling, J. K. M. Sanders, *Inorg. Chem.* **2002**, *41*, 5255; c) E. Stulz, S. M. Scott, A. D. Bond, S. Otto, J. K. M. Sanders, *Inorg. Chem.* **2003**, *42*, 3086; d) E. Stulz, S. M. Scott, Y.-F. Ng, A. D. Bond, S. J. Teat, S. L. Darling, N. Feeder, J. K. M. Sanders, *Inorg. Chem.* **2003**, *42*, 6564.

[10] B. Evans, K. M. Smith, *Tetrahedron Lett.* **1977**, *18*, 3079.

[11] a) K. M. Smith, G. H. Barnett, B. Evans, Z. Martynenko, *J. Am. Chem. Soc.* **1979**, *101*, 5953; b) H. J. Shine, A. G. Padilla, S.-M. Wu, *J. Org. Chem.* **1979**, *44*, 4069; c) A. Giraudeau, L. E. Kahef, *Can. J. Chem.* **1991**, *69*, 1161; d) A. Malek, L. Latos-Grażyński, T. J. Bartczak, A. Zadlo, *Inorg. Chem.* **1991**, *30*, 3222; e) L. Ruhlmann, A. Giraudeau, *Chem. Commun.* **1996**, 2007; f) J. Wojaczyński, L. Latos-Grażyński, W. Hrycyk, E. Pacholska, K. Rachlewicz, L. Szterenberg, *Inorg. Chem.* **1996**, *35*, 6861; g) L. Ruhlmann, A. Giraudeau, *Eur. J. Inorg. Chem.* **2001**, 659; h) L. Ruhlmann, M. Gross, A. Giraudeau, *Chem. Eur. J.* **2003**, *9*, 5085.

[12] For example, see: a) S. G. DiMagno, V. S.-Y. Lin, M. J. Therien, *J. Am. Chem. Soc.* **1993**, *115*, 2513; b) V. S.-Y. Lin, S. G. DiMagno, M. J. Therien, *Science* **1994**, *264*, 1105; c) S. Shanmugathasan, C. K. Johnson, C. Edwards, E. K. Matthews, D. Dolphin, R. W. Boyle, *J. Porphyrins Phthalocyanines* **2000**, *4*, 228; d) A. Nakano, A. Osuka, T. Yamazaki, Y. Nishimura, S. Akimoto, I. Yamazaki, A. Itaya, M. Murakami, H. Miyasaka, *Chem. Eur. J.* **2001**, *7*, 3134; e) F. Odobel, S. Suresh, E. Blart, Y. Nicolas, J.-P. Quintard, P. Janvier, J.-Y. Le Questel, B. Illien, D. Rondeau, P. Richomme, T. Häupl, S. Wallin, L. Hammarström, *Chem. Eur. J.* **2002**, *8*, 3027; f) J. T. Fletcher, M. J. Therien, *J. Am. Chem. Soc.* **2002**, *124*, 4298; g) N. Aratani, H. S. Cho, T. K. Ahn, S. Cho, D. Kim, H. Sumi, A. Osuka, *J. Am. Chem. Soc.* **2003**, *125*, 9668; h) K. Tomizaki, A. B. Lysenko, M. Taniguchi, J. S. Lindsey, *Tetrahedron* **2004**, *60*, 2011.

[13] a) M. M. Khan, H. Ali, J. E. van Lier, *Tetrahedron Lett.* **2001**, *42*, 1615; b) N. P. Redmore, I. V. Rubtsov, M. J. Therien, *Inorg. Chem.* **2002**, *41*, 566; c) T. Takanami, M. Hayashi, F. Hino, K. Suda, *Tetrahedron Lett.* **2003**, *44*, 7353; d) Y. Chen, X. P. Zhang, *J. Org. Chem.* **2003**, *68*, 4432; e) G.-Y. Gao, A. J. Colvin, Y. Chen, X. P. Zhang, *Org. Lett.* **2003**, *5*, 3261; f) G.-Y. Gao, Y. Chen, X. P. Zhang, *Org. Lett.* **2004**, *6*, 1837; g) G.-Y. Gao, A. J. Colvin, Y. Chen, X. P. Zhang, *J. Org. Chem.* **2004**, *69*, 8886.

[14] Quite recently, Arnold and co-workers independently reported the synthesis of *meso*-phosphorylporphyrins based on the Pd-catalyzed C–P cross-coupling reaction. See: a) F. Atefi, O. B. Locos, M. O. Senge, D. P. Arnold, *J. Porphyrins Phthalocyanines*, **2006**, *10*, 176; b) F. Atefi, J. C. McMurtrie, P. Turner, M. Duriska, D. P. Arnold, *Inorg. Chem.*, in press.

[15] F. Odobel, F. Suzenet, E. Blart, J.-P. Quintard, *Org. Lett.* **2000**, *2*, 131.

[16] D. Gelman, L. Jiang, S. L. Buchwald, *Org. Lett.* **2003**, *5*, 2315.

[17] The chemical shifts of the peripheral protons remain almost identical from −10 °C to −50 °C for **2Zn** and from 20 °C to −60 °C for **3Zn**, implying that these compounds exist mostly as dimers in these temperature ranges.

[18] It is well known that the *meso*-phenyl rings of TPP-type porphyrins do not lie in the same plane as the porphyrin ring due to steric repulsion with the neighboring β-protons.

[19] H. E. A. E. Abdallaoui, P. Rubini, P. Tekely, D. Bayeul, C. Lecomte, *Polyhedron* **1992**, *11*, 1795.

[20] X-ray crystal structure data for $(\mathbf{2Zn})_2$: formula $C_{140}H_{178}N_8O_6P_2Zn_2$, triclinic, crystal size $0.20\times0.10\times0.05$ mm, space group $P\bar{1}$, a = 10.5923(14), b = 17.761(2), c = 18.720(2) Å, α = 86.268(8), β = 80.937(8), γ = 74.127(8)°, V = 3344.3(7) Å^3, Z = 1, ρ_{calcd} = 1.123 g cm^{-3}, $2\theta_{max}$ = 136.4°, T = 93.1 K, μ = 1.084 mm^{-1}, T_{min} = 0.947, T_{max} = 0.736, 35256 measured reflections, 11909 independent reflections (R_{int} = 0.081), 714 refined parameters, wR_2 = 0.3378,

$R = 0.1122$ [$I > 2.00\sigma(I)$], GOF = 1.093, max/min residual electron density 2.21/−0.98 e Å^{-3}. CCDC-281481 contains the supplementary crystallographic data for this compound. These data can be obtained free of charge from the Cambridge Crystallographic Data Centre via www.ccdc.cam.ac.uk/data_request/cif.

[21] Zn−O 1.965(10)–1.970(8) Å; P=O 1.486(8)–1.523(12) Å; P-O-Zn 145.0(4)–157.0(7)°: C. A. Kosky, J.-P. Gayda, J. F. Gibson, S. F. Jones, D. J. Williams, *Inorg. Chem.* **1982**, *21*, 3173.

[22] Zn–O 1.896(3)–1.910(3) Å; P=O 1.493(3)–1.507(3) Å; P-O-Zn 147.1(2)–170.1(2)°. See ref. [19].

[23] a) G. Bandori, G. Bortolozzo, D. A. Clemente, U. Croatto, C. Panattoni, *J. Chem. Soc. A* **1970**, 2778; b) J. A. Thomas, T. A. Hamor, *Acta Crystallogr. Sect. C* **1993**, *49*, 355.

[24] P. Jordan, P. Fromme, H. T. Witt, O. Klukas, W. Saenger, N. Krauß, *Nature* **2001**, *411*, 909.

[25] *The Photosynthetic Reaction Center, Vol. 2* (Eds.: J. Deisenhofer, J. R. Norris) Academic Press, San Diego, **1993**.

[26] X-ray crystal structure data for **3Zn**: formula $C_{74}H_{81}N_4OPZn{\cdot}0.5\,H_2O$, monoclinic, crystal size 0.15×0.07×0.02 mm, space group $P2_1/n$ (no. 14), $a = 18.9921(4)$, $b = 9.8546(2)$, $c = 36.1694(9)$ Å, $\beta = 95.8864(8)°$, $V = 6733.8(3)$ Å^3, $Z = 4$, $\rho_{calcd} = 1.132$ g cm^{-3}, $2\theta_{max} = 50.0°$, $T = 103$ K, $\mu = 0.434$ mm^{-1}, $T_{min} = 0.9378$, $T_{max} = 0.9914$, 53301 measured reflections, 11856 independent reflections ($R_{int} = 0.1614$), 745 refined parameters, $wR_2 = 0.1648$, $R = 0.0858$ [$I > 2.00\sigma(I)$], GOF = 1.081, max/min residual electron density 0.581/−0.395 e Å^{-3}. CCDC-609799 contains the supplementary crystallographic data for this compound. These data can be obtained free of charge from the Cambridge Crystallographic Data Centre via www.ccdc.cam.ac.uk/data_request/cif.

[27] a) X. Chi, A. J. Guerin, R. A. Haycock, C. A. Hunter, L. D. Sarson, *J. Chem. Soc. Chem. Commun.* **1995**, 2567; b) K. Funatsu, T. Imamura, A. Ichimura, Y. Sasaki, *Inorg. Chem.* **1998**, *37*, 1798; c) G. Ercolani, M. Ioele, D. Monti, *New J. Chem.* **2001**, *25*, 783.

[28] All attempts to grow single crystals of **3Zn** from hexane/$CHCl_3$ were unsuccessful.

[29] M. Kasha, H. R. Rawls, M. A. El-Bayoumi, *Pure Appl. Chem.* **1965**, *11*, 371.

[30] For discussion about the excitonic coupling of covalently and noncovalently linked porphyrin dimers, see: a) R. R. Bucks, S. G. Boxer, *J. Am. Chem. Soc.* **1982**, *104*, 340; b) A. Osuka, K. Maruyama, *J. Am. Chem. Soc.* **1988**, *110*, 4454; c) B. C. Bookser, T. C. Bruice, *J. Am. Chem. Soc.* **1991**, *113*, 4208.

[31] The absorption spectra, with energies given in cm^{-1}, were deconvoluted into three Gaussian bands and analyzed.

[32] The association constant between ZnTTP and pyridine in toluene has been reported to be 3.3×10^3 M^{-1} at 25 °C. H. Imai, S. Nakagawa, E. Kyuno, *J. Am. Chem. Soc.* **1992**, *114*, 6719.

[33] For instance, the K_a value of **6** was reported to be $\approx10^{11}$ M^{-1} in $CHCl_3$ at 25 °C. See ref. [3 f].

[34] The [monomer]/[dimer] ratios at these concentrations are estimated to be 61:39 to 99:1 for **2Zn** and 18:82 to 91:9 for **3Zn**, respectively, based on the K_a values in Equation (1).

[35] Y. Le Mest, M. L'Her, N. H. Hendricks, K. Kim, J. P. Collman, *Inorg. Chem.* **1992**, *31*, 835.

[36] J. Vasudevan, R. T. Stibrany, J. Bumby, S. Knapp, J. A. Potenza, T. J. Emge, H. J. Schugar, *J. Am. Chem. Soc.* **1996**, *118*, 11676.

[37] M. C. Burla, M. Camalli, B. Carrozzini, G. L. Cascarano, C. Giacovazzo, G. Polidori, R. Spagna, SIR2002, *J. Appl. Crystallogr.* **2003**, *36*, 1103.

[38] P. T. Beurskens, G. Admiraal, G. Beurskens, W. P. Bosman, R. de Gelder, R. Israel, J. M. M. Smits, The DIRDIF-99 Program System, Technical Report of the Crystallography Laboratory, University of Nijmegen (The Netherlands), **1999**.

[39] Crystal Structure 3.7.0, Crystal Structure Analysis Package, Rigaku and Rigaku/MSC, 9009 New Trails Drive, The Woodlands, TX 77381, (USA), **2000–2004**.

[40] D. J. Watkin, C. K. Prout, J. R. Carruthers, P. W. Betteridge, Crystals Issue 10, Chemical Crystallography Laboratory, Oxford (UK), **1996**.

[41] G. M. Sheldrick, SHELX97, University of Göttingen (Germany), **1997**.

Received: June 14, 2006
Published online: October 16, 2006

